

INFLUENCE OF CYCLE NUMBER, TEMPERATURE AND MANUFACTURING PROCESS ON DEFORMATION-INDUCED MARTENSITE IN META-STABLE AUSTENITIC STAINLESS STEELS

D. KALKHOF, M. NIFFENEGGER, M. GROSSE and G. BART
PAUL SCHERRER INSTITUT
NUCLEAR ENERGY AND SAFETY DEPARTMENT
LABORATORY FOR MATERIALS BEHAVIOUR
CH- 5232 VILLIGEN PSI
SWITZERLAND

Referenz: D. Kalkhof, M. Niffenegger, M. Grosse and G. Bart, “**Influence of Cycle Number, Temperature and Manufacturing Process on Deformation-induced Martensite in Meta-stable Austenitic Stainless Steels**”, 5th International Conference on Contribution of Materials Investigation to the Resolution of Problems Encountered in Pressurized Water Reactors (Fontevraud-5), Paper No. 104, pp. 1-12, Fontevraud, France, 23-27. September, 2002.

ABSTRACT

During cyclic loading of austenitic stainless steel, microstructural changes occur, which affect both the mechanical and the physical properties. Typical features are the rearrangement of dislocations and, in some cases, a deformation-induced martensitic phase transformation. In our investigation martensite formation was used as an indication for material degradation due to fatigue. Knowledge about mechanisms and influencing parameters of the martensitic transformation process is essential for the application in a lifetime monitoring system.

The investigations showed that for a given meta-stable austenitic stainless steel the deformation-induced martensite depends on the applied strain amplitude, the cycle number (accumulated plastic strain) and the temperature. It was demonstrated that the volume fraction of martensite continuously increases with the cycle number. Therefore, martensite content could be used for indication of the fatigue usage. According to the Coffin-Manson relation the dependence of the martensite content on the cycle number could be described with a power law. The exponent was determined to be equal to 0.5 for the applied loading and temperature conditions. The influence of temperature on deformation-induced martensite was considered by means of a thermodynamic relation. Furthermore, the initial material state (initial defect density) played an important role for the martensite formation rate.

Material properties and microstructures were characterised by metallography, neutron diffraction, and advanced magnetic non-destructive techniques. In order to investigate the correlation between the martensite content in the austenitic matrix and magnetic properties, the magnetic susceptibility was determined. Furthermore, a high sensitive Giant Magneto Resistant sensor was used to visualise the martensite distribution at the surface of the fatigue specimens. All applied techniques, neutron diffraction and advanced magnetic methods allowed the detection of martensite in the differently fatigued specimens (temperature 20-260 °C with a total strain amplitude of 0.40 % and in cold worked and solution annealed material states).

INTRODUCTION

Degradation of nuclear materials can affect the performance and operational life of nuclear power plants in an essential manner. Monitoring of material degradation is a new trend with the intention to set-up a methodology for a physically based lifetime assessment. It includes the discovery of indications for ageing in the microstructure and the measurement of the influenced mechanical and physical properties. The technical goal consists in the development of a lifetime monitor applied to a specific ageing mechanism and to a certain class of materials.

In view of life extension efforts of nuclear power plants, many investigations are in progress in order to assess the structural integrity of different components. In many cases, this involves unexpected loads, which were not taken into account during design of components, e.g. temperature cycling arising from unforeseen stratification flow conditions. Under certain power plant transients (start-up/shut-down, hot stand-by, thermal stratification) at critical locations of piping and nozzles, material degradation caused by accumulated cyclic plastic strain takes place. Furthermore, the influence of the pressurized hot water environment can reduce the margins to the fatigue crack initiation. However, materials subjected to cyclic loading exhibit changes in microstructure already before macroscopic crack initiation begins, this period covers a considerable part of fatigue life. Existing methods for in-service inspection (ISI) are mainly specialised for crack detection. Advanced non-destructive testing (NDT) methods for monitoring of material degradation are sensitive to any micro-structural changes in the material leading to a degradation of the mechanical properties. Therefore, these indirect methods require a careful interpretation of the measured signal in terms of micro-structural evolutions due to ageing.

Transformation of austenite to martensite is the basic reaction in the hardening of carbon steels, but it plays also an important role in the mechanical working of austenitic steels, and is often encountered in practice as an unusual work hardening. Martensite transformation is diffusionless and it occurs primarily on cooling. The temperature M_s , at which it starts is independent on the cooling rate. Transformation can be made to occur at temperatures above M_s under the influence of mechanical stresses and strains [1,2]. Scheil investigated an iron-nickel alloy containing 29 % of nickel, and found that the amount of martensite increased with the degree of cold working and decreased with increasing working temperature. Angel was the first who studied comprehensively the isothermal formation of martensite induced by plastic deformation in austenitic stainless steels as a function of stress, strain and deformation energy [3]. He discovered that at room and elevated temperatures the dependence of the martensite content with the plastic strain is nearly linear and for temperatures less than room temperature there is a stimulating effect in the beginning of tensile straining and a stabilizing effect during the later stages of transformation. A thermodynamical criterion for the martensite formation was proposed by Patel and Cohen, taking into consideration the contribution of deformation energy to the Gibbs potential [4]. The kinetics of strain-induced martensitic nucleation has been modeled by Olson and Cohen [5]. They assume that nucleation occurs preferentially at intersecting shear bands which consist of bundles of faults, twins and hcp ϵ -martensite. The morphology of the transformation product is typically described as lath-like [6]. Investigation of deformation-induced martensite under low-cycle fatigue (LCF) conditions was presented by Baudry and Pineau [7]. The influence of the plastic strain amplitude and temperature on the martensite content was qualitatively described. Bayerlein et al. [8] indicated the phases which were formed during LCF of AISI 304L stainless steel as ϵ - and α' -martensite by electron diffraction pattern analysis. In situ observations by transmission electron microscopy have provided further information about this process. Suzuki et al. [9] have found that dislocations arranged in pile-ups help to promote the transformation. In high chromium alloy stainless steels, e.g. AISI 304, α' -martensite has been found far away from any shear band.

In spite of an improved understanding of the deformation-induced martensite in austenitic steels the knowledge about the influencing parameters especially under cyclic loading is not satisfying, since in most studies the tests have been carried out in a narrow temperature range or at few temperature values. Furthermore, there is a lack of information about the correlation between the mechanical response, martensite formation and the microstructural processes. One reason is the difficulty of measuring the martensite distribution on the surface and in the bulk of the fatigue samples. Here advanced diffraction methods using neutron and synchrotron light sources offer new possibilities [10]. For technical application advanced magnetic techniques (Giant Magneto Resistance sensor GMR [11], Super-conducting Quantum Interference Device SQUID [12]) are now available to transfer the knowledge to field experiments. The investigations described in this paper are primarily aimed to analyse the influencing parameters of the deformation-induced martensite formation during fatigue. The experimental work contributes to the development of a lifetime monitor system for fatigue damage at austenitic stainless steel components.

EXPERIMENTAL PROCEDURES

Material and manufacturing process

For investigation of the influencing parameters on the deformation-induced martensite, series of LCF specimens were fabricated. Materials used were heats of titanium stabilised austenitic steel X6CrNiTi18-10 corresponding to the German grade 1.4541 (equivalent to AISI 321) chosen for their relevance in nuclear power plant piping and because of their instable properties of the austenitic phase. The material as received was analysed by means of Inductive Coupled Plasma Emission Photometry (ICP-OES) within an uncertainty of 2% of the measured value (Table 1).

Table 1: Chemical composition in wt.-% of X6CrNiTi18-10 heat A and B.

| | C | Cr | Ni | Ti | Si | Mn | P | S | Mo | Co |
|---------------|-------|-------|------|-------|-------|-------|-------|-------|-------|-------|
| Heat A | 0.022 | 17.70 | 9.84 | 0.148 | 0.381 | 1.850 | 0.029 | 0.022 | 0.334 | 0.118 |
| Heat B | 0.020 | 17.05 | 9.60 | 0.140 | 0.450 | 1.880 | 0.028 | 0.030 | 0.320 | 0.100 |

Two heats with different fabrication and heat treatment conditions were used. In Table 2 the fabrication conditions and the mechanical properties for both heats are summarized. Heat A was delivered in form of cold drawn bars with a diameter of 20 mm. Before the cold drawing process the material was solution annealed and then quenched in water. Heat B consists of warm drawn bars with a diameter of 30 mm. In order to homogenize the microstructure, heat B was additional solution annealed in a vacuum chamber and afterwards quenched in oil.

Table 2: Fabrication conditions and mechanical properties of X6CrNiTi18-10 heat A and B.

| | Fabrication | Heat treatment | Yield strength | Ultimate strength |
|---------------|--|--|----------------|-------------------|
| Heat A | Solution annealing (4 h at 1040 °C, quenched in water) Cold drawing | None | 430 MPa | 625 MPa |
| Heat B | Warm drawing | Solution annealing (1 h at 1040 °C quenched in oil) | 170 MPa | 580 MPa |

Turning and mechanically polishing the surface gave the shape of the specimens. In Fig. 1 the design of the applied LCF specimen is shown. After mechanical straining, investigations were concentrated on the 20 mm long polished cylindrical part of the specimen.

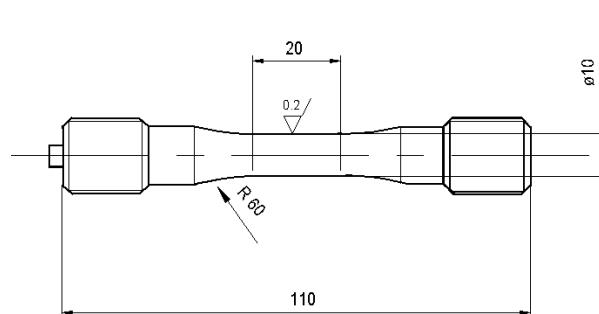


Figure 1: Low-cycle fatigue specimen according to ASTM E 606

Mechanical test conditions

Standard tensile specimens with a diameter of 10 mm were strained with a strain rate of 10^{-3} s^{-1} up to a certain level of plastic strain. Fatigue testing was performed by applying a strain controlled sinusoidal alternating loading ($R = -1$) at room and elevated temperatures up to $260 \text{ }^\circ\text{C}$. For all LCF tests a total strain amplitude of 0.40 % was applied. A climatic chamber was used for both experiments at elevated temperatures as well as for room temperature tests. To keep the specimen temperature constant during LCF loading, the surface temperature was continuously measured whereas the ambient temperature was controlled. For the loading frequency of 1.0 Hz and the total strain amplitude of 0.40 % the temperature measured at the surface of the specimen was $70 \text{ }^\circ\text{C}$. To obtain results for room temperature, the frequency had to be reduced to 0.5 Hz. Different usage factors were realised by varying cycle numbers of strain loads. The usage factor D was defined to be equal to 1.0 for specimens, where crack initiation had already occurred. Crack initiation was decided to take place if the force drop reached 2 % of the maximum force amplitude in the saturation region. For specimens without a crack, D was defined as the ratio of the applied cycle number to an averaged cycle number representing crack initiation. This averaged value for crack initiation was obtained in pre-testing on 3-5 specimens for each test temperature.

Neutron diffraction method

In meta-stable austenitic steels some amount of the austenitic face centred cubic (fcc) lattice can change to a body centred cubic (bcc) lattice. Due to lattice parameters the Bragg's reflections of austenite and martensite occur at different scattering angles. Therefore the quantitative determination of martensitic content is possible by using diffraction techniques. Since neutrons have a relatively large penetration depth (in the order of cm) the powder diffractometer (DMC) at the neutron spallation source SINQ at the Paul Scherrer Institute was used to determine the martensitic content. The instrument is optimised for high intensity. It allows the determination of the phase content down to values below 1 %. With a neutron beam wave length of $\lambda = 0.38 \text{ nm}$, a range of the scattering angle 2θ of $68^\circ \leq 2\theta \leq 147^\circ$ was analysed. Measurements on the LCF specimens were performed with a beam cross section of 40 mm (width) x 10 mm (height). The measuring position was in the middle of the LCF specimens ($\pm 5 \text{ mm}$ in height). During measurement the specimen was continuously turned around the axis to average a possible inhomogeneous distribution of martensite in the samples.

Magnetic measurement techniques

While austenite is paramagnetic, the generated martensite is ferromagnetic. Therefore cyclic loading also influences the magnetic properties, which can be characterised with several parameters. Among the magnetic parameters the susceptibility represents the magnetic conductivity, which is increased during the fatigue testing due to the micro-structural formation of ferromagnetic martensite needles. In order to investigate the correlation between martensitic content, magnetic susceptibility and the usage factor, the susceptibility was determined by means of an instrument called FERROMASTER[®]. The instrument contains a permanent magnet to partially magnetise the specimen and two pick-up coils to measure the change of magnetisation caused by a change of the applied magnetic field. It is calibrated to yield the susceptibility in a range from 0.0000 to 1.0000.

Furthermore a high sensitive Giant Magneto Resistant (GMR) sensor was used to visualise the martensite distribution at the surface of the LCF specimens. A special manipulator that allows the scanning of the specimens was applied. The equipment worked in an eddy current mode and was calibrated using a set of special tensile specimens made for calibration.

RESULTS AND DISCUSSION

Mechanical behaviour of X6CrNiTi18-10 under LCF loading

The mechanical behaviour of meta-stable austenitic stainless steels has been found to be changed by martensitic transformation. In Fig. 2 the typical stress amplitude versus cycle number curves for total strain controlled LCF tests at the temperature of 70 °C are shown. The material behaviour is characterised by a hardening in the first 10 cycles followed by a softening during the next 1000 cycles. From about 1000 cycles up to crack initiation a second hardening was observed.

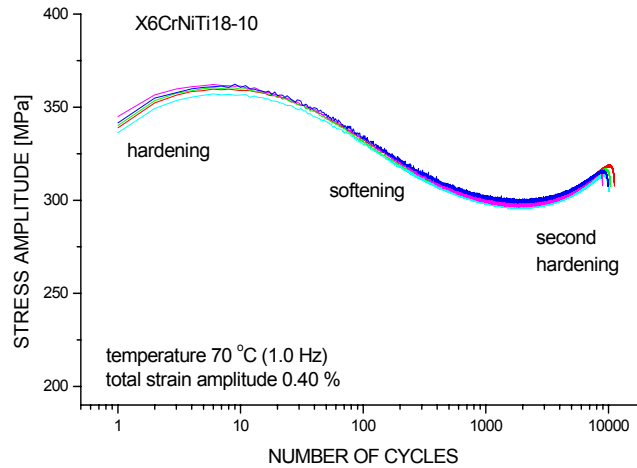


Figure 2: Typical stress amplitude vs. cycle number curves (log scale) for cyclic loading (heat A) at a temperature of 70 °C (1.0 Hz).

The measurements of the volume fraction of α' -martensite during tensile [3] and fatigue tests [13] has confirmed that a direct relation exists between second hardening and martensite transformation. In tensile tests the transformation has been found to be triggered by a certain amount of plastic strain, which depends on the material and on the temperature. In fatigue tests the plastic strain amplitude is the decisive parameter [14].

The following influences on the mechanical behaviour and the deformation-induced martensite formation during LCF loading were systematically investigated for the initial material states of heat A and B:

- cycle number representing a certain value of accumulated plastic strain
- temperature

Effect of cycle number

Our intention to perform tensile experiments was firstly to compare results for quasi-static and cyclic loading and secondly to create an ensemble of specimens to be used for calibration of the non-destructive methods. The results presented in Fig. 3 are in agreement with [3] that there is a linear correlation between the volume fraction of martensite formed and the plastic tensile strain applied at room temperature. A simple expression for this dependency makes it easy to predict the martensite content for a certain strain level. This linear correlation is also very advantageous for the calibration procedure of NDT methods.

$$x_m = x_{mo} + 0.3 \cdot \varepsilon_{plastic} \quad (1)$$

valid for X6CrNiTi18-10 (heat A, $\sigma_Y = 430$ MPa), x_m and x_{mo} are martensite contents for the strained and the initial material state. $\varepsilon_{plastic}$ is the plastic strain value.

The fatigue tests were performed under total strain controlled test conditions with a total strain amplitude of 0.40 %. The test frequency of 1.0 Hz results in a heating of the specimens up to 70 °C measured at the surface. Data sets with and without crack initiation were produced. The dependence of the martensite content on the cycle number is shown in Fig. 4. In LCF testing the Coffin-Manson law describes the correlation between the plastic strain amplitude and the cycle number to failure. It is confirmed in Fig. 4 that the accumulated plastic strain correlates with the volume fraction of martensite. According to the Coffin-Manson relation, the martensite data can be fitted with a power law. From data analysis the exponent was determined to be equal to 0.5. Consequently, the dependence of the martensite content on the cycle number can be described by a square root function for the investigated material X6CrNiTi18-10 (heat A).

$$x_m = x_{mo} + 0.31 \cdot \frac{\epsilon_{plastic}}{2} \cdot \sqrt{N} \quad (2)$$

valid for X6CrNiTi18-10 (heat A, $\sigma_Y = 430$ MPa) and $T = 70$ °C. $\epsilon_{plastic}$ is the plastic strain range. The plastic strain amplitude for data in Fig. 4 was 0.24 %.

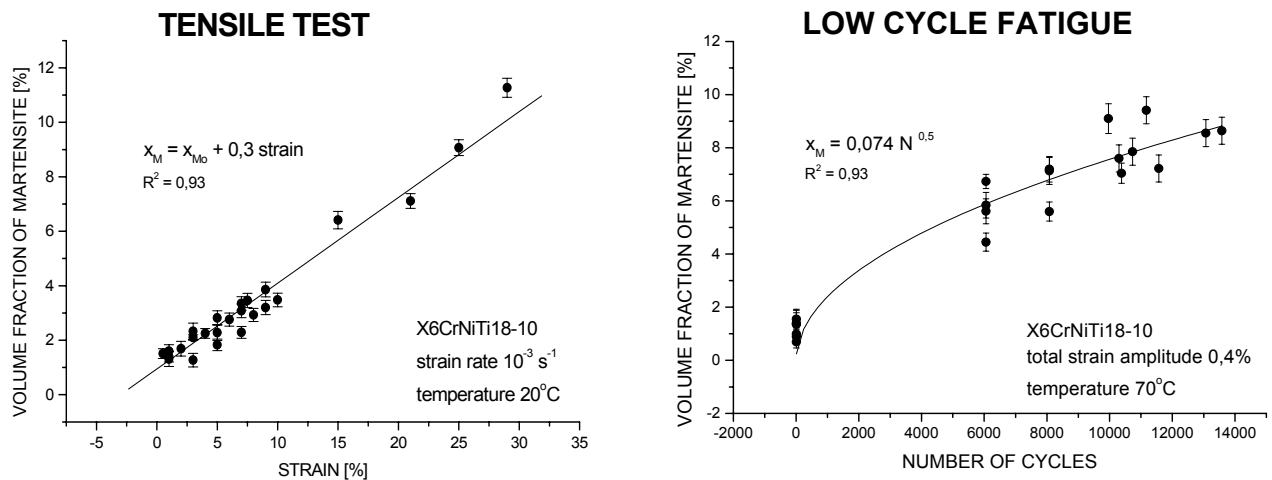


Figure 3: Formation of martensite by plastic tensile strain.

Figure 4: Formation of martensite by accumulated plastic strain.

Effect of temperature

Since the driving force for martensite transformation is the degree of undercooling $T_0 - T$, where T_0 is the equilibrium temperature, the test temperature has a strong influence on the course of transformation. Fig. 5 and 6 illustrate this temperature dependency in the mechanical behaviour for quasi-static straining and LCF of the austenitic stainless steel X6CrNiTi18-10 (heat A). Stress-strain curves for tensile testing at various temperatures showed that there is a relatively large gap between 20 °C and 60 °C. This implied a strong change in the martensite formation rate between these temperatures. The stress amplitude of cyclic straining at various deformation temperatures is plotted in Fig. 6. The different rise of second hardening suggested that the martensite formation rate is continuously decreasing with increasing temperature. The stress amplitude increase at second hardening was larger in the temperature range of 20 °C up to 70 °C than above. For higher temperatures material behaviour showed even a second softening.

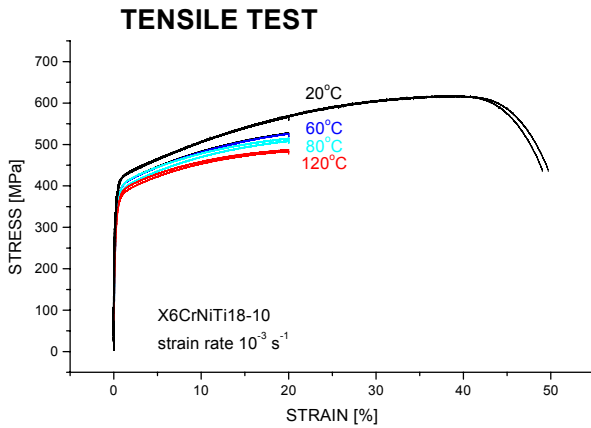


Figure 5: Typical stress-strain curves for uniaxial tensile straining (heat A) at various deformation temperatures.

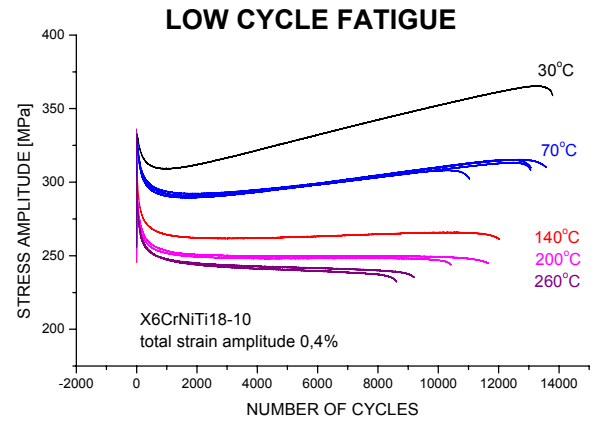


Figure 6: Typical stress amplitude vs. cycle number curves for cyclic loading (heat A) at various deformation temperatures.

The martensite transformation process can be described thermodynamically. The free energy change has to be large enough for the reaction to mount the activation barrier between the austenitic and the martensitic states. For the spontaneous reaction this happens at the M_s temperature. Above M_s but below the equilibrium temperature T_0 there is a supply of free energy available, which however is insufficient to initiate transformation. The additional energy required may be supplied as mechanical energy, e.g. by uniaxial tension or by LCF. As the free energy change decreases with increasing temperature, the martensite content should show a corresponding decrease. This has been confirmed experimentally (Fig. 7 and 8). To investigate the temperature dependent martensite formation the tensile straining was stopped at a defined level of plastic strain (20 %). In the case of low cycle fatigue the results were referred to a temperature dependent number of cycles. To exclude an additional martensite contribution caused by crack initiation, data for the usage factor of $D = 0.8$ were analysed. In dependence on temperature, cycle numbers varied from 9'720 cycles at 200 °C up to 10'730 cycles at 60 °C.

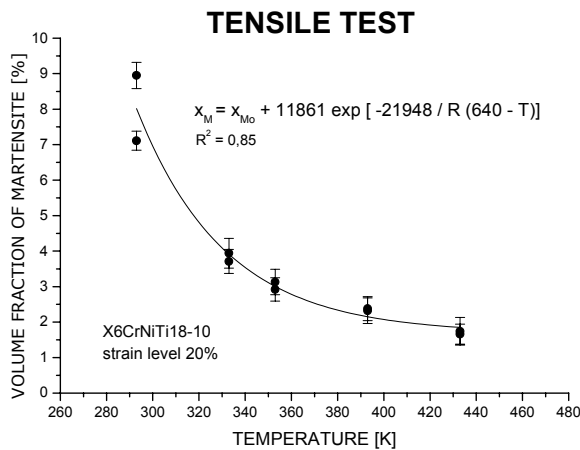


Figure 7: Temperature dependence of martensite content at tensile straining. Plastic strain level 20 %. Strain rate 10^{-3} s^{-1} .

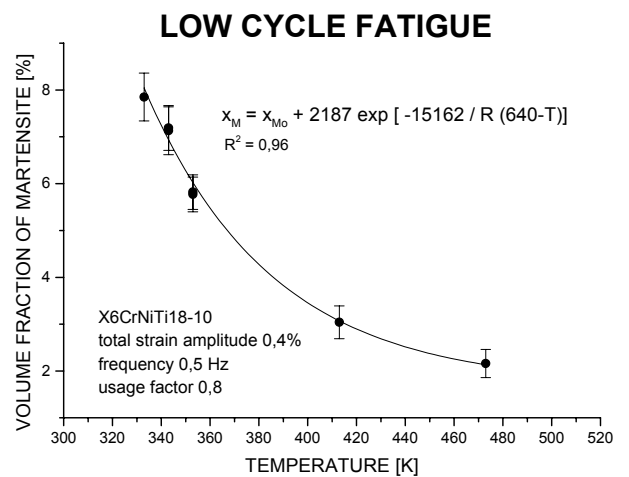


Figure 8: Temperature dependence of martensite content for cyclic loading. Total strain amplitude 0.40 %. Frequency 0.5 Hz. Usage factor $D = 0.8$.

The temperature dependent martensite data can be analysed using a thermodynamic relation as follows:

$$x_m = x_{m_0} + A \cdot \exp[-Q / R(T_0 - T)] \quad (3)$$

where x_m and x_{m_0} are the volume fractions of martensite for the strained and initial state of material, Q is the load dependent activation energy in kJ / mol, T_0 the equilibrium temperature, R the gas constant in J / K mol and A is a material and load specific parameter. Angel calculated the temperature dependent free energy change accompanying the martensitic transformation for a 18-8 chromium-nickel steel and found that T_0 is about 640 K [3]. Using T_0 from Angel the following activation energies and A -parameters for tensile straining and LCF were found:

Tensile straining: $Q = 22 \text{ kJ/mol}$; $A \approx 12'000$; X6CrNiTi18-10 (heat A, $\sigma_y = 430 \text{ MPa}$), $\epsilon_{\text{plastic}} = 20 \%$

LCF: $Q = 15 \text{ kJ/mol}$; $A \approx 2'000$; X6CrNiTi18-10 (heat A, $\sigma_y = 430 \text{ MPa}$), $\Delta\epsilon_{\text{total}} = 0.40 \%$, $D = 0.8$

Consequently, it was demonstrated that the temperature dependence of the deformation-induced martensite can be characterised by a thermodynamically based expression for both quasi-static loading and low cycle fatigue.

Effect of manufacturing process

The influence of the manufacturing process and heat treatment (initial material state) on the martensite formation rate was investigated for 2 heats of the X6CrNiTi18-10 austenitic stainless steel representing different initial densities of micro-structural defects. Heat A represented a cold worked material and heat B a solution annealed state.

It can be assumed that due to the additional solution annealing for heat B the density of initial micro-structural defects like stacking faults, dislocations and twins was reduced to a lower level. Consequently, the decrease of the initial micro-structural defect density leads to a relatively low yield strength of 170 MPa (room temperature). Due to a large number of dislocations caused by the cold working process the yield strength of heat A is relatively high (430 MPa). Typical stress-strain curves for both heats obtained at room temperature and at the strain rate of 10^{-3} s^{-1} are shown in Fig. 9. The mechanical behaviour in tensile testing of heat A representing a high defect density was characterised by high strength and low ultimate strain, whereas heat B showed lower strength and higher ultimate strain.

Intersections of shear bands in meta-stable austenites have been shown to be effective sites for deformation-induced martensitic nucleation. For heat A the dislocation density and consequently the number of shear bands and the probability for shear band intersection is higher than for heat B. Assuming that a) shear band intersection is the dominant mechanism of martensite nucleation and b) dislocation pile-ups promote the transformation, a different behaviour of the martensite formation for heats A and B can be expected.

The obtained martensite formation rate during cyclic loading for both heats is illustrated in Fig. 10. The LCF tests were performed with a frequency of 1.0 Hz at room ambient temperature and with a total strain amplitude of 0.40 %. The temperature measured at the surface of the specimens was 70 °C. The number of cycles corresponded to the usage factors of 0.6, 0.8, 1.0. The initial content of martensite was 0.7-1.6 vol.% for heat A. No initial martensite was found in heat B. According to the Coffin-Manson relation the cycle number dependence of the martensite content for heat A followed a square root function, the dependence for heat B showed a linear behaviour. It was surprising that the influence of the initial material state on the martensite formation rate was very strong. The cold working led to a final martensite content of about 9 vol.% at crack initiation ($D = 1.0$) whereas for the solution annealed material the final volume fraction of martensite was only about 3 vol.%. The cycle numbers (referred to the 2 % load drop) were much higher for the annealed specimens (26'000 - 63'000 cycles) than for the specimens with cold working (9'300 - 13'500 cycles). The results confirmed that the initial micro-structural defects play an important role for the martensite formation rate. Otherwise it showed that the knowledge about the initial material state is essential to predict the martensite content for a certain cycle number.

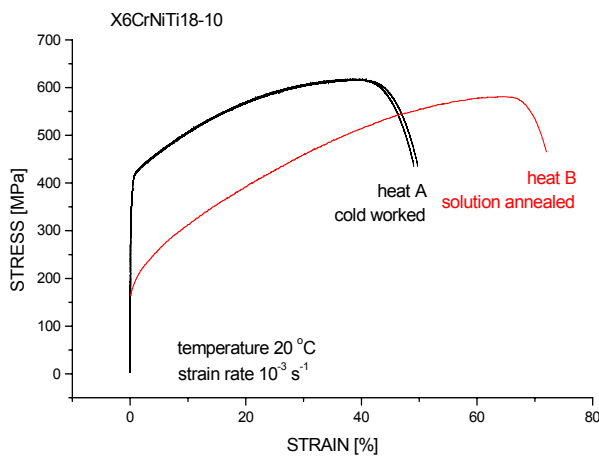


Figure 9: Stress-strain curves of tension testing for different heats of the austenitic steel X6CrNiTi18-10 at room temperature and at a strain rate of 10^{-3} s^{-1} .

Heat A: cold working material state.

Heat B: solution annealed material state.

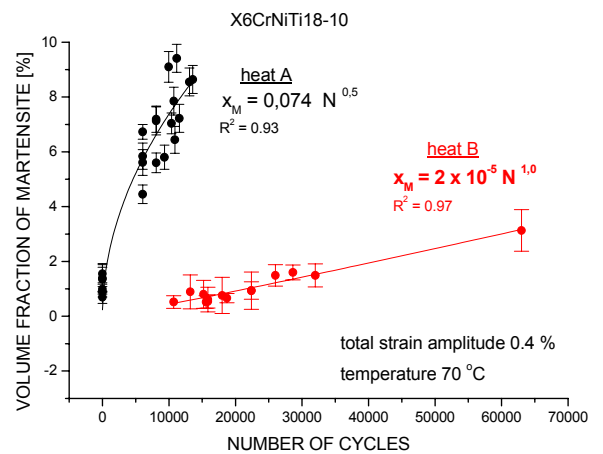


Figure 10: Volume fraction of martensite formed during LCF tests at 70 °C (1.0 Hz) for different heats of X6CrNiTi18-10.

Plastic strain amplitude 0,24 %.

Heat A: cold working material state.

Heat B: solution annealed material state.

Measurement of magnetic susceptibility

For the detection of material degradation due to low-cycle fatigue in austenitic stainless steels advanced magnetic techniques can be used. The instrument FERROMASTER[®] is designed for the measurement of small ferromagnetic amounts in a paramagnetic matrix. A typical application of the instrument is the determination of the remaining δ -ferrite in austenitic materials and welds. The device is calibrated to yield the susceptibility (magnetic conductivity) in a range from 0.0000 to 1.0000. Therefore, in the case of deformation-induced martensite in the austenitic matrix the instrument can be applied if the martensite content is below 10 vol.%. The measuring instrument was calibrated using special calibration samples for which the susceptibility was known. Then detection of changes of susceptibility in the LCF specimens was possible and an increase of the volume fraction of martensite resulted in a corresponding increase of susceptibility. This is illustrated in Fig. 11 for the ensemble of calibration specimens strained in tensile testing. The martensite content of the tensile specimens for calibration was generated by certain amounts of plastic strain using the correlation (1). A linear correlation between susceptibility and martensite content was found.

Results of susceptibility measured at the LCF specimens are shown in Fig. 12. For comparison the dependence of the martensite content obtained by neutron diffraction was added. Trends of both martensite content and susceptibility were the same. Therefore, the dependence of susceptibility on cycle number can be described by a square root function, see equation (2). Furthermore, the measurements of susceptibility might substitute the neutron diffraction examination. For one material state it was demonstrated that the determination of the fatigue usage in austenitic stainless steels could be carried out by means of measurement of the magnetic susceptibility.

Concerning the scatter of the data it can be stated that the scatter-band of the neutron diffraction data was larger than for the magnetic measurements. The penetration depths of both measuring techniques are different. The sensitivity of neutron diffraction decreases with the penetration depth whereas for the FERROMASTER[®] it increases up to a depth of 10 mm. Therefore, measurements of both methods are influenced by the martensite distribution at the surface and in depth in a different manner. Special experiments are needed to visualise the axial and radial distribution of martensite.

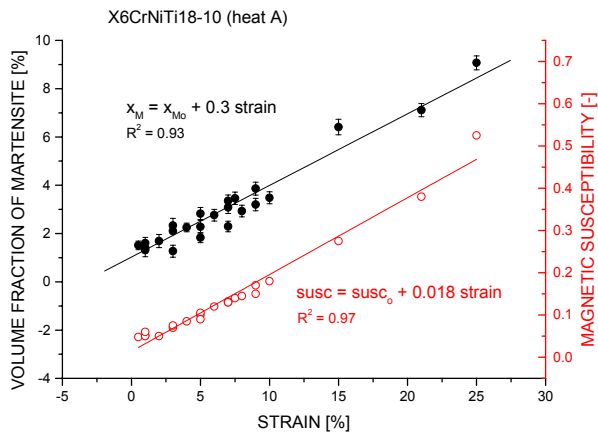


Figure 11: Dependency of both martensite content and magnetic susceptibility on the tensile plastic strain for the ensemble of calibration specimens.

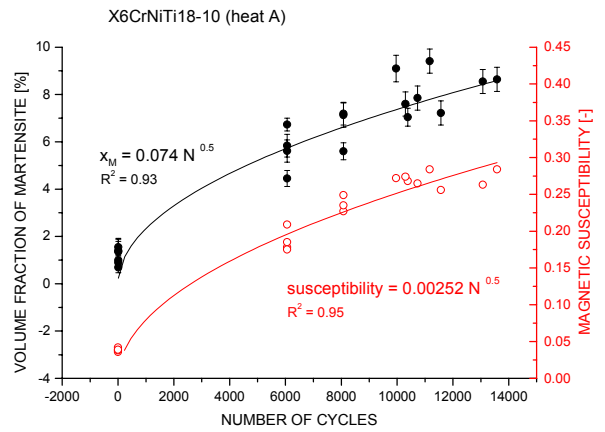


Figure 12: Dependency of both martensite content and magnetic susceptibility on cycle number for LCF specimens tested at the total strain amplitude of 0.40%, frequency 1.0 Hz and temperature 70 °C.

Imaging of martensite distribution using GMR magnetic technique

By means of a GMR sensor measurements of the martensite distribution with high local resolution were performed. The measuring technique was calibrated with the ensemble of tensile specimens containing a certain amount of martensite. The GMR magnetometer works in the eddy current (EC) mode. The measured EC impedance depends on several physical and geometrical parameters, e.g. distance between sensor and specimen, design and size of the specimen, local differences in the electric and magnetic conductivities. The martensite in the austenitic matrix influences both the electric and magnetic conductivity. Using the high local resolution of the sensor a visualisation of the martensite distribution at the surface of the fatigue specimens was possible. For investigations sensors from Nonvolatile Electronics Inc., USA and an EC measuring system developed in the Fraunhofer Institute of Non-Destructive Testing, Germany were used.

After fatigue tests some specimens were scanned using the GMR magnetometer. Examples for the as received material state and for the usage factor of $D = 0.8$ are shown in Fig. 13 and 14. The image of martensite for the initial material state showed a more or less homogeneous distribution. In circumferential direction the martensite was distributed homogeneously. In axial direction a little more martensite was found at the ends of the specimens (transition of cylindrical part to radius), probably caused by fabrication processes. The martensite distribution image of the fatigued specimens (Fig. 14) was quite different to that of the as received state. After fatigue with $D = 0.8$ the martensite is concentrated in certain areas located in the middle of the specimen. It can be expected that crack initiation will take place at these critical positions. In order to investigate the influence of cycle number, temperature and heat treatment on the deformation-induced martensite, it is important to determine mean values for the volume fraction of martensite. Therefore, it is essential to rotate the specimen during laboratory test measurements. But more experiments for imaging radial and axial martensite distribution are needed to reduce the uncertainties in the measuring techniques and to better understand the course of the martensite formation.

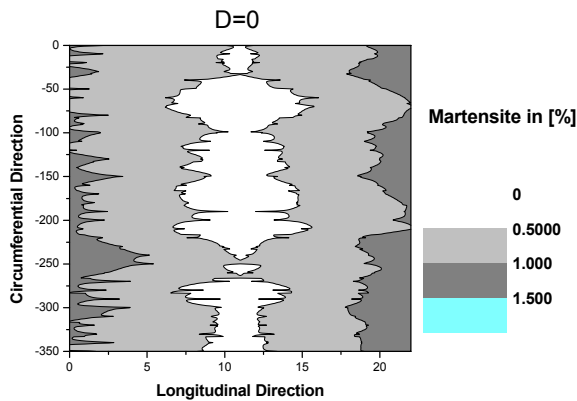


Figure 13: Martensite distribution at the surface of the fatigue specimens. Example for initial material state.

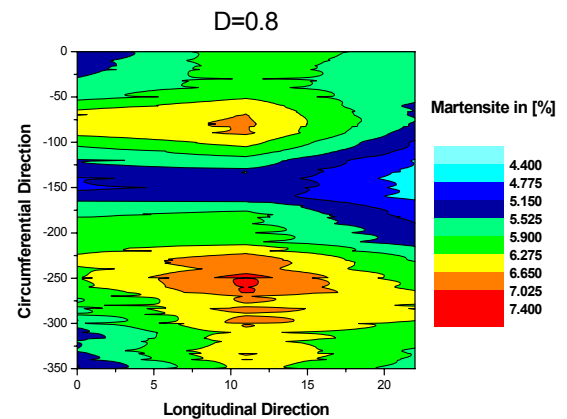


Figure 14: Martensite distribution at the surface of the fatigue specimens. Example for $D = 0.8$. Total strain amplitude 0.40 %. Temperature at the surface 70 °C (1.0 Hz).

SUMMARY AND CONCLUSIONS

The influence of cycle number, temperature and heat treatment on the deformation-induced martensite formation was investigated. Tensile and low-cycle fatigue specimens were strained and fatigued to defined plastic strain levels and usage factors. Two heats of titanium stabilised austenitic stainless steel X6CrNiTi18-10 corresponding to the German grade 1.4541 (equivalent to AISI 321) were investigated and different manufacturing and heat treatment conditions were realised, e.g. cold working (heat A) and solution annealing (heat B). Test series were performed at room temperature and at elevated temperatures up to 260 °C.

Correlations were found between the volume fraction of martensite, the plastic strain value (tensile test) and the number of cycles (LCF). This showed that deformation-induced martensite can be used as an indication of material degradation due to tensile straining or LCF in meta-stable austenitic stainless steels. The LCF material behaviour was characterised by a hardening in the first 10 cycles followed by a softening during the next 1000 cycles. From about 1000 cycles up to crack initiation a second hardening was observed. It was confirmed that the second hardening was caused by martensite formation. The mean cycle numbers representing crack initiation ($D = 1.0$) for the total strain amplitude of 0.40 % were determined as follows:

- Heat A: 13'800 (30 °C) / 11'700 (70 °C) / 11'500 (200 °C),
- Heat B: 28'000 (70 °C) / 19'000 (200 °C).

The corresponding volume fraction of martensite was measured by means of neutron diffraction (mean values):

- Heat A: 15.5 vol.% (30 °C) / 9.0 vol.% (70 °C) / 2.5 vol.% (200 °C),
- Heat B: 2.5 vol.% (70 °C) / 0.8 vol.% (200 °C).

Since the driving force for martensite transformation is the degree of undercooling below the equilibrium temperature, the test temperature has a strong influence on the course of transformation. Experimental results showed that martensite content continuously decreases with increasing temperature. It was shown that the temperature dependence of the deformation-induced martensite could be described by a thermodynamically based expression for both quasi-static loading and LCF.

Summarising results for the influencing parameters a general equation for the deformation-induced martensite formation for a given austenitic material is proposed as follows:

$$x_m = x_{m0} + A^* \cdot \frac{\Delta \varepsilon_{plastic}}{2} \cdot \sqrt{N} \cdot \exp[-Q / R(T_o - T)] \quad (4)$$

where x_m and x_{m0} are volume fractions of martensite for the strained and initial state of material, $\Delta \varepsilon_{plastic} / 2$ is the load amplitude, N the cycle number, Q the material and load dependent activation energy in kJ / mol, T_o the equilibrium temperature, R the gas constant in J / K mol and A^* a material and load specific parameter.

Measurements with magnetic methods have shown the strong relation between martensitic content and the magnetic susceptibility. Susceptibilities from 0.05 up to 0.6 in tension specimens and from 0.04 up to 0.28 in the LCF specimens were measured and a linear relation between martensitic content and susceptibility was determined. A special handling device for scanning the surface of the specimens with a Giant Magneto Resistant sensor was built and tested. First measurements were successful and the distribution of martensite could be visualised. The volume fraction of martensite obtained by neutron diffraction experiments was used to calibrate the GMR technique. Neutron diffraction appeared to be the appropriate tool to serve as a calibration method for the deformation-induced martensite in the LCF specimens. All applied methods, neutron diffraction and advanced magnetic techniques allowed the detection of martensite in the differently fatigued specimens (temperature 20-260 °C with a total strain amplitude of 0.40 % and in cold worked and solution annealed material states).

ACKNOWLEDGMENT

The financial support for this work by the Swiss Federal Nuclear Safety Inspectorate (HSK) and the Swiss Federal Office of Energy (BFE) is gratefully acknowledged. Thanks are also expressed to E. Groth for the performing of the mechanical tests.

REFERENCES

- [1] E. Scheil, *Zeitschrift für anorganische und allgemeine Chemie* 207 (1932), 21-40
- [2] K. Mathieu, *Mitteilungen aus dem Kaiser-Wilhelm-Institut für Eisenforschung* 24 (1942), 243-248
- [3] T. Angel, *Formation of martensite in austenitic stainless steels*, J. Iron and Steel Institute 177 (1954), 165
- [4] J.R. Patel and M. Cohen, *Acta Metall.* 1 (1953), 531-538
- [5] G.B. Olson and M. Cohen, *Kinetics of strain-induced martensitic nucleation*, Metallurgical Transactions A 6A (1975), 791
- [6] P.M. Kelly and J. Nutting, *J. Iron Steel Institute* 184 (1961), 199
- [7] G. Baundry and A. Pineau, *Influence of strain induced martensitic transformation on the low-cycle fatigue behaviour of a stainless steel*, Mater. Sci. Eng. 28 (1977), 229
- [8] M. Bayerlein, H.-J. Christ und H. Mughrabi, *Plasticity induced martensitic transformation during cyclic deformation of AISI 304L stainless steel*, Mater. Sci. Eng. A 114 (1989), 11
- [9] T. Suzuki, H. Kojima, K. Suzuki, T. Hashimoto, S. Koike and M. Ichihara, *Acta Metall.* 10 (1976), 353
- [10] D. Kalkhof, M. Grosse, M. Niffenegger, D. Stegemann, W. Weber, *Microstructural investigations and monitoring of degradation of LCF damage in austenitic steel X6CrNiTi18-10*, Proc. Int. Conf. on Fatigue of Reactor Components, EPRI 1006070, June 2001
- [11] M.A. Lang, *Non-destructive evaluation of deformation-induced martensite formation of austenitic steel X6CrNiTi18-10 by means of high sensitive magnetometers*, dissertation, University of Saarbrücken, 2000
- [12] M. Otaka, S. Evanson, K. Hasegawa, K. Takaku, *Detection of thermal aging degradation and plastic strain damage for duplex steel using SQUID-sensor*, SMIRT 11, Transactions Vol. L (1991), 459
- [13] H.-J. Bassler and D. Eifler, *Characterisation of plasticity-induced martensite formation during fatigue of austenitic steel*, Low-Cycle Fatigue and Elasto-Plastic Behaviour of Materials, ed. by K.-T. Rie and P.D. Portella, Elsevier Science Ltd. 1998
- [14] M. Grosse, M. Niffenegger, D. Kalkhof, *Monitoring of low-cycle fatigue degradation in X6CrNiTi18-10 austenitic steel*, J. of Nuclear Materials 296 (2001) 305-311